OPEN ACCESS
CellPress

Cell Reports
Article

# Dominant Lethal Pathologies in Male Mice Engineered to Contain an X-Linked DUX4 Transgene

Abhijit Dandapat,[1,2,7] Darko Bosnakovski,[1,2,7,8] Lynn M. Hartweck,[1,2] Robert W. Arpke,[1,2] Kristen A. Baltgalvis,[3] Derek Vang,[4] June Baik,[1,6] Radbod Darabi,[1,6] Rita C.R. Perlingeiro,[1,6] F. Kent Hamra,[5] Kalpna Gupta,[4] Dawn A. Lowe,[3] and Michael Kyba[1,2,*]

[1]Lillehei Heart Institute, University of Minnesota, 2231 6th Street SE, Minneapolis, MN 55455, USA
[2]Department of Pediatrics, University of Minnesota, 2231 6th Street SE, Minneapolis, MN 55455, USA
[3]Program in Physical Medicine and Rehabilitation, University of Minnesota, 420 Delaware Street SE, Minneapolis, MN 55455, USA
[4]Vascular Biology Center, Division of Hematology, Oncology, and Transplantation, Department of Medicine MMC 480, 420 Delaware Street SE, University of Minnesota, Minneapolis, MN 55455, USA
[5]Department of Pharmacology, Cecil H. and Ida Green Center for Reproductive Biology Sciences, University of Texas Southwestern Medical Center, 5323 Harry Hines Boulevard, Dallas, TX 75390, USA
[6]Department of Medicine, University of Minnesota, 312 Church Street SE, Minneapolis, MN 55455, USA
[7]Co-first author
[8]Present address: University Goce Delčev-Štip, Faculty of Medical Sciences, Krste Misirkov b.b., 2000 Štip, R. Macedonia
*Correspondence: kyba@umn.edu
http://dx.doi.org/10.1016/j.celrep.2014.07.056


## SUMMARY

**Facioscapulohumeral muscular dystrophy (FSHD) is an enigmatic disease associated with epigenetic alterations in the subtelomeric heterochromatin of the D4Z4 macrosatellite repeat. Each repeat unit encodes *DUX4*, a gene that is normally silent in most tissues. Besides muscular loss, most patients suffer retinal vascular telangiectasias. To generate an animal model, we introduced a doxycycline-inducible transgene encoding *DUX4* and 3′ genomic DNA into a euchromatic region of the mouse X chromosome. Without induction, DUX4 RNA was expressed at low levels in many tissues and animals displayed a variety of unexpected dominant leaky phenotypes, including male-specific lethality. Remarkably, rare live-born males expressed *DUX4* RNA in the retina and presented a retinal vascular telangiectasia. By using doxycycline to induce DUX4 expression in satellite cells, we observed impaired myogenesis in vitro and in vivo. This mouse model, which shows pathologies due to FSHD-related D4Z4 sequences, is likely to be useful for testing anti-DUX4 therapies in FSHD.**

## INTRODUCTION

Facioscapulohumeral muscular dystrophy (FSHD) is a common degenerative myopathy caused by illicit recombination within D4Z4, a subtelomeric macrosatellite repeat on chromosome 4 (van Deutekom et al., 1993; Wijmenga et al., 1992). Array contractions cause chromatin changes (de Greef et al., 2009; Gabellini et al., 2002; van Overveld et al., 2003; Zeng et al., 2009) but cause disease only on a specific allele of chromosome 4, termed 4qA161 (Lemmers et al., 2004, 2007). FSHD nonpermissive alleles, and related D4Z4 repeats on chromosome 10 (Bakker et al., 1995; Deidda et al., 1996), lack an ATTAAA polyadenylation sequence downstream of the terminal repeat (Dixit et al., 2007; Lemmers et al., 2010). These data suggest that repeat contractions result in an mRNA transcript produced from D4Z4, which must be polyadenylated to cause disease.

The D4Z4 transcript bears an open reading frame encoding a double homeodomain protein named DUX4 (Gabriëls et al., 1999), and this protein is specifically expressed, albeit extremely weakly, in FSHD (Dixit et al., 2007; Snider et al., 2010). Expression of DUX4 at very low levels interferes with myogenesis and sensitizes cells to oxidative stress (Bosnakovski et al., 2008a). These low-level effects are intriguing as defects in myogenic gene expression (Celegato et al., 2006; Winokur et al., 2003a) and sensitivity to oxidative stress (Turki et al., 2012; Winokur et al., 2003b) have been detected in FSHD muscle and primary cell cultures. High levels of DUX4 expression cause rapid cell death in vitro (Bosnakovski et al., 2008a; Kowaljow et al., 2007).

In addition to muscle wasting, most individuals afflicted with FSHD have subclinical retinal vascular pathologies involving vascular tortuosity, microaneurysms, occlusions, and occasionally small exudates (Fitzsimons et al., 1987; Padberg et al., 1995).

A transgenic mouse has recently been described that carries an insertion of tandem arrays of a 2.5-unit FSHD allele. Although transcription could be detected in several tissues, and very rare DUX4+ nuclei were detected in cultured cells from this animal (Krom et al., 2013), the animal was normal except for an eye keratitis that developed with age. With the aim of studying the effect of DUX4 expression in vivo, we generated mice with a doxycycline (dox)-inducible *DUX4* transgene upstream of hypoxanthine phosphor-ribosyl transferase (*HPRT*) on the X chromosome. Unexpectedly, in the absence of dox, these animals display a variety of pathologies. We characterize these pathologies and use this model to investigate effects of D4Z4/DUX4 expression on myogenic progenitor cell activity.

## RESULTS

To generate a dox-inducible, DUX4-expressing mouse, we used inducible cassette exchange recombination (Bosnakovski et al., 2008a; Iacovino et al., 2011) to insert a genomic DNA fragment encoding the DUX4 open reading frame and 3′ sequences from the terminal D4Z4 repeat up to the *Eco*RI site into a euchromatic site on the X chromosome. This site, upstream of a functional *HPRT* gene, was chosen for its ability to give reliable transgene expression (Bronson et al., 1996; Cvetkovic et al., 2000; Portales-Casamar et al., 2010; Touw et al., 2007). The integration places this genomic DNA into a dox-inducible locus regulated by a second generation, tight, tet-response element (Agha-Mohammadi et al., 2004). The reverse tetracycline transactivator for the Tet-On system is expressed ubiquitously from Rosa26 (Hochedlinger et al., 2005). The integration vector provides an SV40 poly A signal downstream of the inserted DNA. We named this transgene iDUX4(2.7), because DUX4 is on a 2.7 kb genomic fragment (Figure 1A).

### The iDUX4(2.7) Transgene Is Male-Specific Dominant Lethal

Blastocyst injection generated chimeric males with poor transmission of the transgene: only two F1 progeny were obtained after 1 year of mating chimeras to C57BL/6 females. These carrier females displayed a striped mosaic scaly skin, mild alopecia phenotype. They transmitted the transgene to female progeny, but most litters lacked male carriers (Figure 1B), demonstrating that the DUX4(2.7) transgene behaved as a male-specific dominant embryonic lethal. Evaluation of embryonic litters at embryonic day 14.5 (E14.5) revealed male carrier fetuses with various degrees of developmental delay (Figure 1C). Rarely, carrier males survived to birth, and these animals were runted, displayed the skin phenotype homogeneously, and invariably died before 2 months of age. Notably, when carrier males survived to term, they were usually of similar size to littermate controls at birth. The runting and the skin phenotypes usually became apparent within a few days but were sometimes not initiated until the second week (Figure 1D), and by 6 weeks, iDUX4(2.7) males were significantly underweight (Figure 1E). On histological examination, the skin was found to have excessive numbers of cells, in both the epidermis and dermis (Figures 1F and 1G), features that may explain the flaky scaly skin, and alopecia. We evaluated various tissues from affected males for leaky expression of the transgene (Figure 1H). Unexpectedly, expression in skin, as in most other tissues, was very low and inconsistently detected at 38 cycles of RT-PCR. Nor did we detect the DUX4 protein in any tissues in the absence of dox. This situation is very reminiscent of patients with FSHD, in which spliced RNA transcripts from the terminal D4Z4 element can be detected by RT-PCR in most samples but protein is exceedingly difficult to detect.

However, DUX4 mRNA was consistently detected in testis, retina, and brain. DUX4 has been detected in normal human testis (Snider et al., 2010), and FSHD patients present retinal vascular defects; therefore, we evaluated these tissues in greater detail. Compared to sibling controls, testes of 42-day-old iDUX4(2.7) males displayed a marked defect in gametogenesis. Seminiferous tubule cross sections showed almost complete loss of spermatocytes during late prophase in most tubules. This resulted in relatively few tubules that contained round haploid spermatids and a lack of elongating spermatids compared to wild-type (WT) siblings (Figures 2A and 2B).

To evaluate retinae, we generated montages of z stack laser-scanning confocal microscopy images of retinal whole mounts stained with PECAM antibody. The iDUX4(2.7) males displayed features associated with telangiectasia: excessive branching with looping and twisted retinal vessels, which appear more dilated than control retinae (Figures 2C and 2D). Morphometric analysis of these images revealed a dramatic increase in vessel branching (nodes), as well as significant increases in vessel length and overall density of vessels in iDUX4(2.7) males compared to controls (Figures 2E–2G), suggestive of increased neovascularization.

### iDUX4(2.7) Males Have Proportionally Weaker Muscles but Show No Evidence of Muscular Dystrophy prior to 6 Weeks of Age

Muscles of the iDUX4(2.7) males were smaller than those of their matched sibling controls and fibers were fewer and smaller; however, muscles did not become overtly dystrophic within the short lifespan of these mice (Figure 3A). Grip-strength measurements revealed that the iDUX4(2.7) males were much weaker than sibling controls, but strength was proportional to body size (Figure 3B). We measured the force-generation capacity of isolated extensor digitorum longus (EDL) and soleus muscles. Both muscles produced much lower absolute force; however, when normalized to muscle cross-sectional area, the specific force-generating capacity was not significantly different from WT (Figures 3C and 3D). Soleus muscle fiber type distribution, based on myosin heavy chain isoform expression (types 1, 2a, and 2x), was not different between iDUX4(2.7) and wild-type mice (Figure 3E).

### Demethylation of DUX4 in Myogenic and FAP Progenitors from Muscle

To determine whether the integrated transgene more resembled an FSHD-associated or a WT allele, we evaluated methylation of the transgene in rare live-born iDUX4(2.7) males by bisulfite sequencing. We initially evaluated testis and hind limb muscle, tissues with visualizable versus barely detectable DUX4 mRNA. Remarkably, in both tissues, the transgene was completely demethylated (Figure 4A). We then initiated cultures of total muscle mononuclear cells and subsequently fluorescence-activated cell sorting (FACS) purified and subcultured the $\alpha$7-integrin$^-$ PDGFR$\alpha^+$ fibroadipogenic (FAP) (Joe et al., 2010; Uezumi et al., 2010) and the $\alpha$7-integrin$^+$ PDGFR$\alpha^-$ myoblast fractions. The transgene was likewise completely demethylated in both progenitor cell types (Figures 4A and S1).

### Biased X Inactivation in Females

We then investigated methylation in females, using peripheral blood samples of female iDUX4(2.7) heterozygous breeders. In stark contrast to males, sequences from females indicated that the gene could be in one of two states: either similar to that seen in males or heavily methylated. This is consistent with X inactivation, which, when it occurred on the

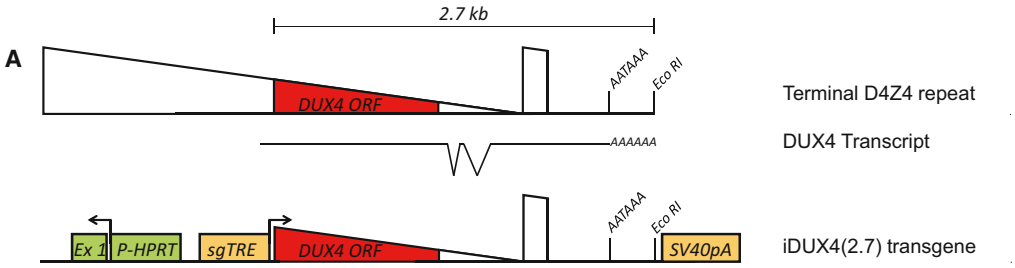


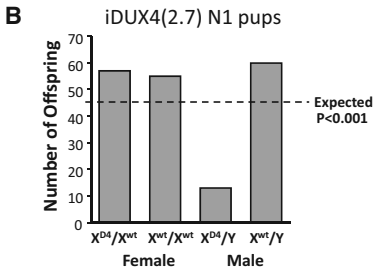


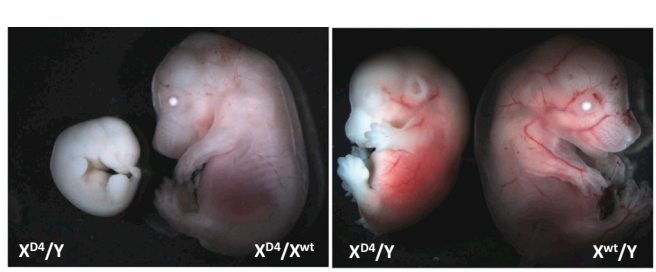



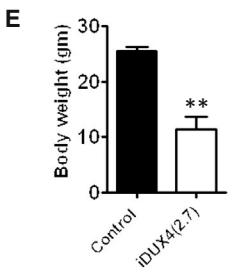


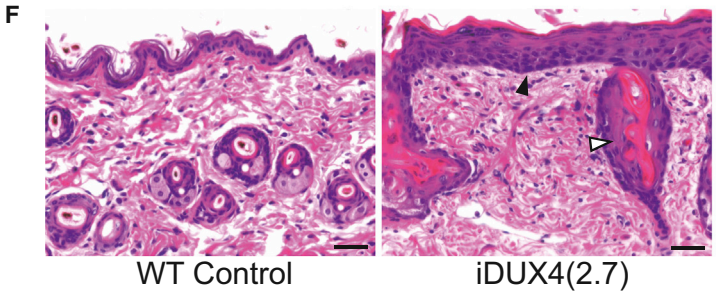


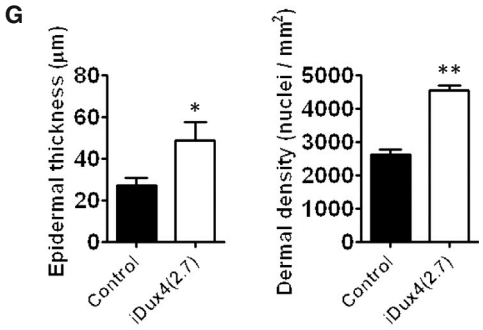


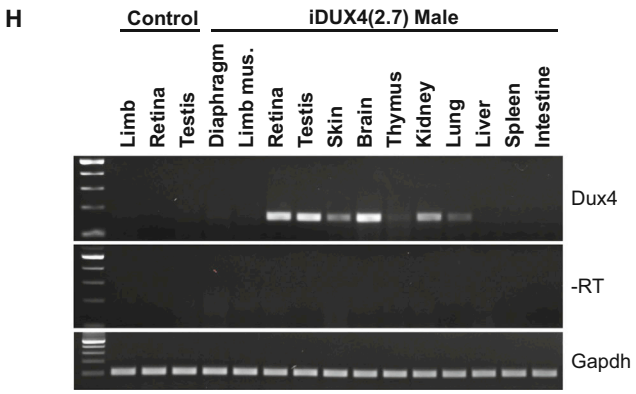


(legend on next page)

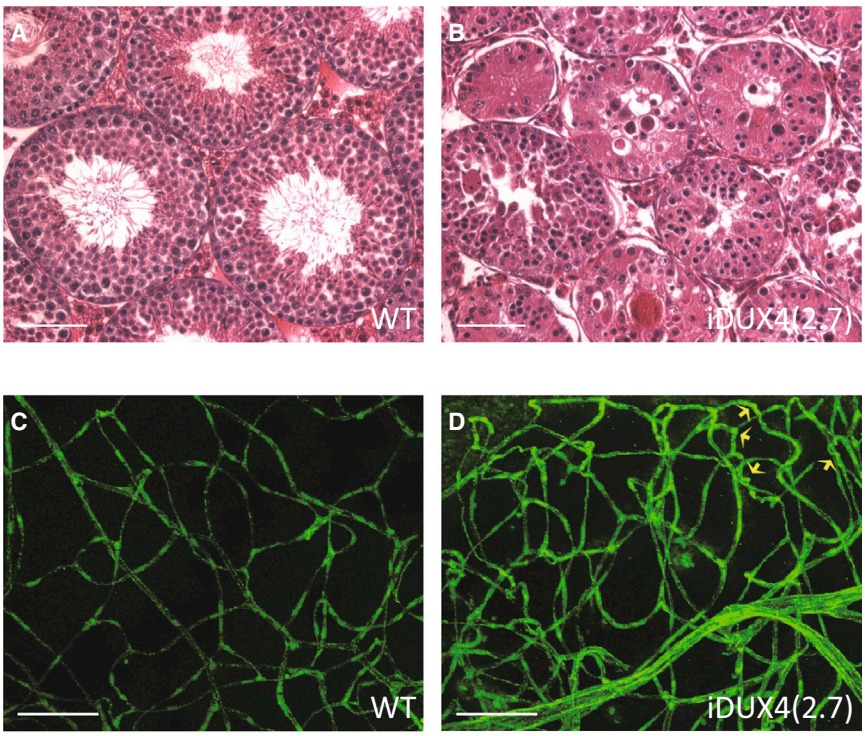


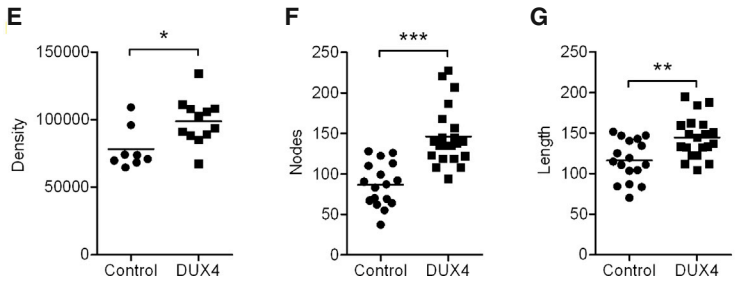


**Figure 2. Phenotypes in Testis and Retina**

(A) Cross section through WT seminiferous tubules. The scale bar represents 50 μm.

(B) Cross section through iDUX4(2.7) seminiferous tubules.

(C) Vasculature in WT retina: montage of z stack laser scanning confocal microscopy images of retina flat mounts stained with anti-CD31/PECAM showing normal presentation of vasculature. The scale bar represents 50 μm.

(D) Vasculature in iDUX4(2.7) retina showing dense network of disorganized and twisted/looping vessels. Yellow arrows indicate twisted vessels.

(E) Morphometric analysis of retinal images following skeletonization showing vascular density measured as immunoreactive pixels ($p < 0.05$).

(F) Morphometric quantification of vessel branching measured by nodes ($p < 0.001$).

(G) Morphometric quantification of total vessel length. For (E)–(G), each point represents values/field, averaged from three to four different fields per retina; n = 7 iDUX4, n = 8 WT ($p < 0.01$).

DUX4-bearing X, would result in high levels of methylation. Because X inactivation is random, an equal proportion of the two states is expected. Remarkably, the methylated sequences greatly outnumbered the demethylated sequences in females (Figure 4B). This X inactivation bias strongly suggests that there is selection against cells that inactivate the WT X, leading female heterozygotes to be composed mainly of cells in which the DUX4-bearing X was inactivated.

## Expression of DUX4 in Muscle-Derived Progenitors

In contrast to the difficulty of detecting DUX4 transcript in primary muscle tissue, the DUX4 transcript was detectable at low levels in both myoblasts and FAPs (Figure 4C). Notably, in iDUX4(2.7) cultures, the FAP population predominated prior to FACS and isolated iDUX4(2.7) myoblasts had a clear growth disadvantage compared to their WT controls, whereas iDUX4(2.7) FAPs showed no growth disadvantage (Figure 4D). We next sought to detect the DUX4 protein in isolated myoblasts and FAPs. We found no detectable protein expression in FAPs (not shown); however, myoblast cultures consistently showed scattered cells with nuclear DUX4 protein (Figure 4E), similar to what was seen with the D4Z4 mouse (Krom et al., 2013). The protein could also be

**Figure 1. The iDUX4(2.7) Transgene Is Male-Specific Dominant Lethal**

(A) Schematics of the terminal D4Z4 repeat (above), the DUX4 transcript with introns and proposed AATAAA polyadenylation signal (below), and the construct integrated into the X chromosome (bottom). HPRT, hypoxanthine phosphor-ribosyl transferase; Ex1, exon 1; sgTRE, second-generation tet-response element.

(B) Genotypes of live pups from iDUX4(2.7) female carriers bred to WT males and chi-square p values.

(C) iDUX(2.7) embryos at E14.5. $X^{D4}$ indicates the transgenic iDUX4(2.7)-bearing chromosome. Most male carrier embryos display severe growth delay or resorption.

(D) Examples of litters with runted iDUX4(2.7) males. Left: a P5 litter with two obvious runts and one animal, identified by arrowhead, with some hair loss that later became runted. Right: littermate WT and iDUX4(2.7) males at P28.

(E) Weight at 6 weeks, $p < 0.05$.

(F) H&E staining of skin. Note the hypertrophic epithelium (filled arrowhead) and the abnormal glands (open arrowhead). The scale bar represents 20 μm.

(G) The epidermal thickness and nuclear density in the dermis were measured at six locations per section and averaged (*$p < 0.04$; **$p < 0.001$), and the experiment was repeated with three mice.

(H) RT-PCR detection of the DUX4 transcript in tissues of iDUX4(2.7) transgenic male mice. Robust and repeatable expressions were always seen in the brain, retina, and testis. Other tissues displayed sporadic and weaker expression.

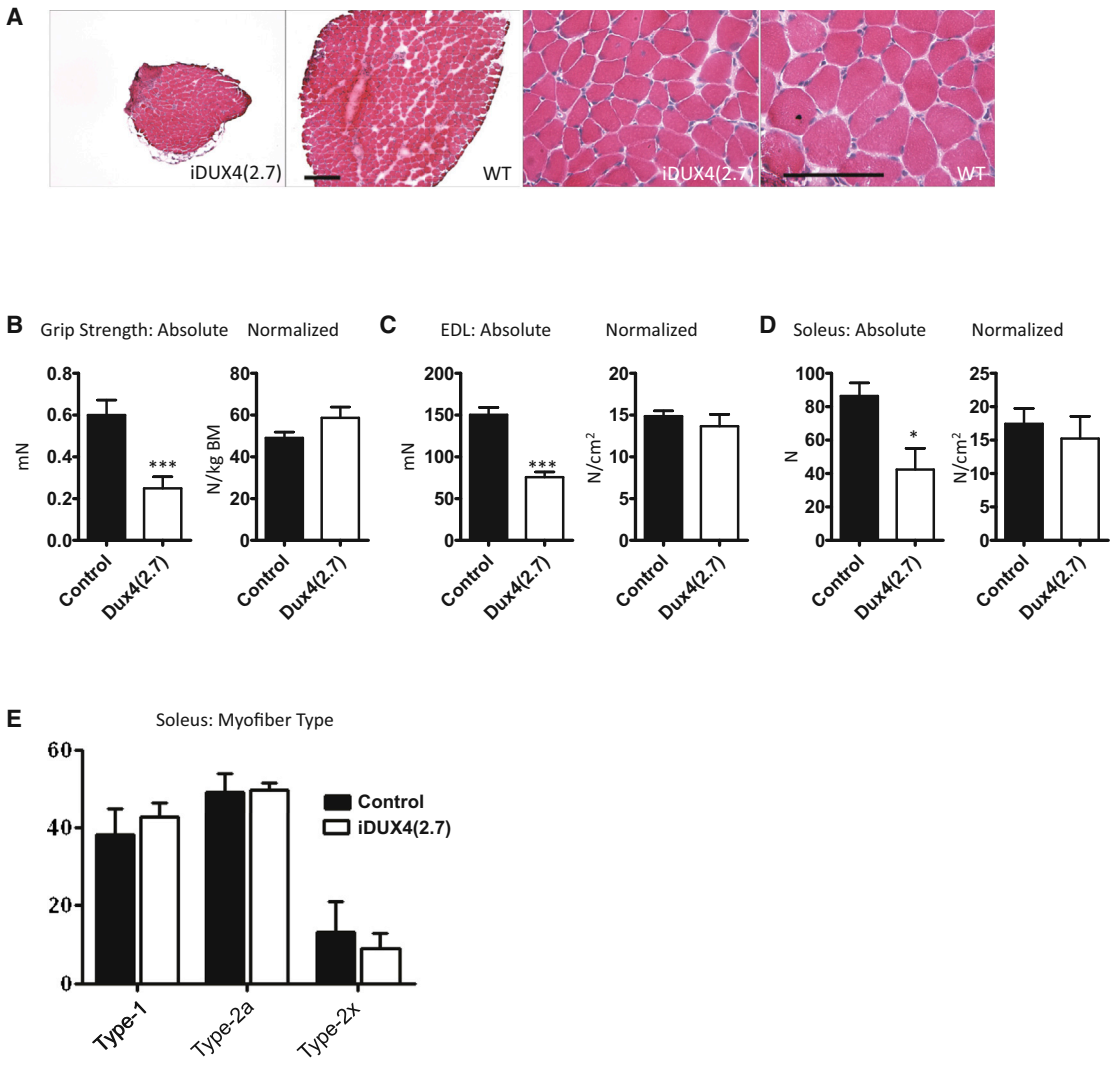


**Figure 3. Muscle in iDUX4(2.7) Animals**

(A) H&E staining of cross sections through soleus muscles of iDUX4(2.7) males (left) and male littermate controls (right). The scale bar represents 100 μm (low-magnification images) or 200 μm (high-magnification images).

(B) Grip strength measurements at 6 weeks: absolute at left ($p < 0.001$) and normalized to body mass at right ($n = 4$).

(C) Maximal isometric force generated by the extensor digitorum longus muscle at 6 weeks: absolute at left ($p < 0.001$) and normalized to cross-sectional area at right ($n = 4$).

(D) Maximal isometric force generated by the soleus muscle at 6 weeks: absolute at left ($p = 0.026$) and normalized to cross-sectional area at right ($n = 4$).

(E) Fiber-type analysis based on myosin heavy chain isoform expression.

detected, and at greater frequency, in nuclei from differentiated myotubes, often in groups of adjacent nuclei. Quantification revealed that about 5% of myonuclei from differentiated cultures stained DUX4+, whereas in the myoblast cultures, DUX4 protein was present in about 1.5% of nuclei (Figure 4F). This result is not necessarily suggestive of greater expression in differentiated cultures: myotubes are syncitia, therefore active DUX4 transcription in one nucleus can lead to uptake and positive staining of nuclear proteins in nearby myonuclei (Block et al., 2013; Tassin et al., 2013), so at the same frequency of expression, myotubes are predicted to have greater numbers of positive nuclei than myoblasts. Indeed, a careful comparison of two independent myoblast and myotube cultures revealed very similar levels of expression at the RNA level before versus after differentiation (Figure 4G), although it is important to point out that these results are nonquantitative. The lack of detectable protein in most nuclei by immunostaining, as well as the lack of detectable protein in FAPs, may indicate the sensitivity of the assay is limiting. Indeed, between laboratories, the immunohistochemical method has produced widely varying estimates of frequencies of nuclei positive for DUX4 in FSHD (and control) myoblasts (Jones et al., 2012; Snider et al., 2010).

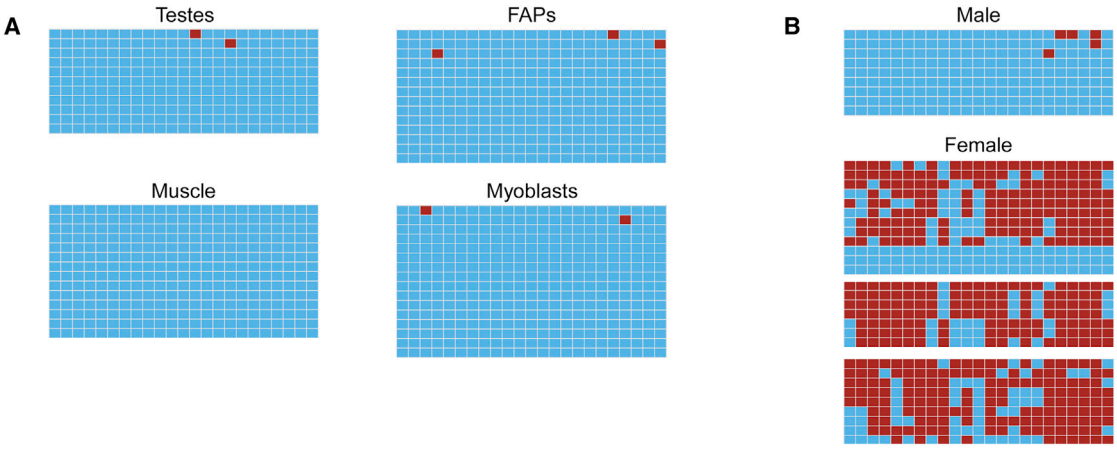


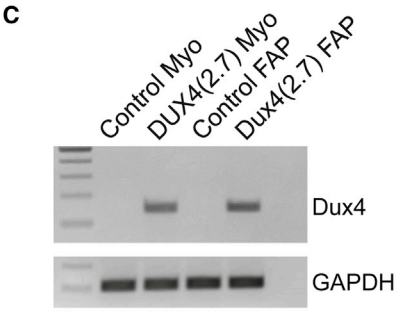


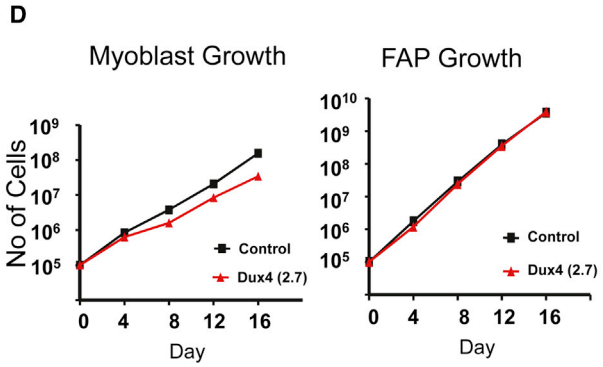


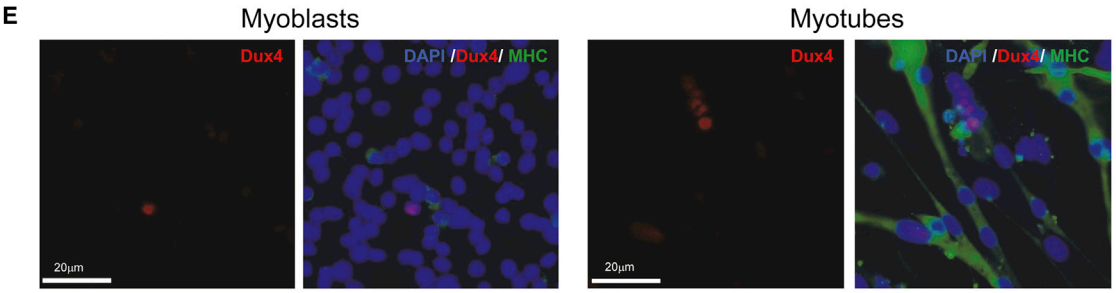


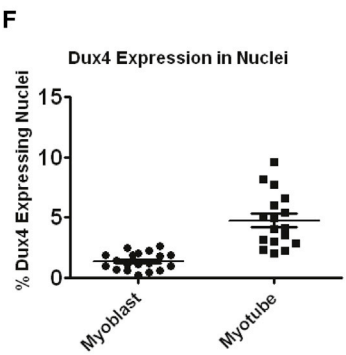


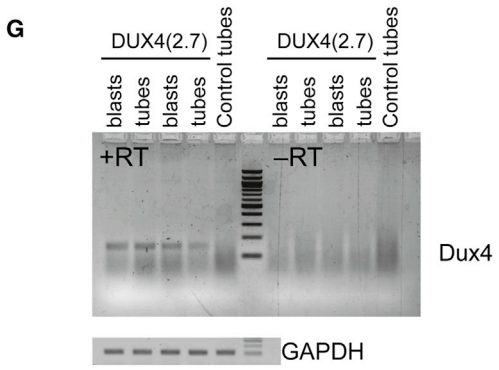


*(legend on next page)*

### Induced DUX4 Expression Is Selectively Deleterious to Myogenic Progenitors

The studies described above were undertaken in the absence of dox; therefore, phenotypes are due to extremely low-level, leaky expression. To evaluate the utility of dox-mediated DUX4 expression, we tested whether the inducible locus was functional by treating myoblast and FAP cultures with a high dose of dox (500 ng/ml) for 24 hr. This confirmed that the inducible system was indeed working as expected: DUX4 protein was expressed in response to dox (Figure 5A). We then subjected ex vivo cultures of myoblasts and FAPs to various lower concentrations of dox. In both myoblasts and FAPs, expression of DUX4 was deleterious; however, growth inhibition was more severe in myoblasts (Figures 5B and 5C).

Low, nontoxic levels of DUX4 expression were shown to interfere with the differentiation of C2C12 myoblasts (Bosnakovski et al., 2008a). To determine DUX4 effects on primary cells, we induced differentiation of myoblasts (into myotubes) and FAPs (into adipocytes) in the presence of low levels of dox (50 ng/ml). Myotube formation was clearly impaired by DUX4 expression, whereas adipocyte differentiation was unaffected (Figure 5D).

### DUX4 Impairs Myogenic Regeneration In Vivo

To test the effect of DUX4 expression during myogenic regeneration in vivo, we transplanted 1,800 FACS-isolated satellite cells from hind limb muscle of iDUX4(2.7) mice into preinjured, irradiated tibialis anterior muscles of NSG-mdx$^{4Cv}$ mice (Arpke et al., 2013). The recipients lack dystrophin; thus, the amount of donor muscle tissue produced by the transplanted cells can be quantified by immunostaining for dystrophin. We found that treatment of mice with 5 mg/kg doxycycline severely impaired the ability of donor satellite cells to produce new muscle (Figures 6A and 6B). This indicates that DUX4 expression is deleterious to muscle regeneration in vivo.

## DISCUSSION

FSHD is one of the most enigmatic of the muscular dystrophies, and despite many efforts, there is no genetic model that displays any phenotype for this disease. In humans, reduction in repeat number (or second-site mutation in rare noncontraction cases; i.e., FSHD2; Lemmers et al., 2012), clearly leads to an epigenetic alteration at D4Z4 (van Overveld et al., 2003) that impairs repeat-induced silencing allowing D4Z4 transcription (Block et al., 2013; Jones et al., 2012; Snider et al., 2009). Although a recently described mouse bearing randomly integrated tandem D4Z4 repeats from an FSHD allele showed some expression of D4Z4 transcript (Krom et al., 2013), this animal did not present profound pathologies. With the recognition that DUX4 has potent myogenesis-relevant phenotypes even at very low levels of expression in C2C12 cells (Bosnakovski et al., 2008a), we sought to generate an animal model based on low-level regulated and systemic expression of DUX4. Systemic expression is relevant because D4Z4 misexpression in FSHD has not been shown to be restricted to myoblasts or muscle fibers. Indeed, the presence of nonmuscle phenotypes such as retinal vascular pathology (Fitzsimons et al., 1987; Gieron et al., 1985; Small, 1968) and sensorineural hearing loss (Brouwer et al., 1991; Lutz et al., 2013) in FSHD patients, the syndrome of phenotypes associated with very severe infantile FSHD cases with extremely short D4Z4 arrays (Chen et al., 2013), together with the demonstration of epigenetic changes also in the blood cells of FSHD patients (Hartweck et al., 2013; van Overveld et al., 2003), suggests that misexpression is not restricted to muscle and might be a global feature. Remarkably, in our allele, we found that low-level leaky and variable expression led to several severe phenotypes, making the iDUX4(2.7) mouse an animal model in which FSHD allele-specific DNA has been integrated into the genome and caused a serious pathology.

This pathology is dominant, like FSHD, but dramatically more potent, resulting in male-specific lethality. In humans, the D4Z4 repeats are embedded in subtelomeric heterochromatin and subject to repeat-induced silencing, whereas in this mouse model, the transgene has been inserted into euchromatin and is present in only a single copy. Thus, D4Z4 has lost both the opportunity for repeat-induced silencing as well as its normal heterochromatic genomic environment, both changes that would be predicted to render the transgene more potent than 4q35-linked FSHD alleles (Figure 7). This may explain why the DUX4 transgene has a much stronger dominant-lethal phenotype in this mouse model than in human patients with FSHD. It may also explain the presence of phenotypes in unexpected tissues, for example, skin; however, vector-specific sequences may also contribute to tissue-specific aspects of the leakiness, for example, the minimal promoter might be leaky in skin cells, whereas the endogenous human D4Z4 might not show skin expression. For obvious reasons, outside of muscle biopsies, a careful analysis of tissues in which DUX4 expression can be

**Figure 4. Methylation and DUX4 Expression in Primary Cells**

(A) Methylation of the iDUX4(2.7) transgene in various tissues and primary muscle cells. Bisulfite-treated DNA was amplified by PCR, cloned, and sequenced. Blue boxes indicate unmethylated cytosines of CpG dinucleotides, and red boxes indicate methylated cytosines along the PCR product.

(B) Methylation of the transgene in male and female peripheral blood. One male aged 6 weeks and three independent females aged 6, 9, and 36 weeks are shown. Methylated sequences in females were greatly overrepresented compared to the 1:1 ratio predicted by X inactivation for a heterozygous female ($p = 0.0$).

(C) RT-PCR detection of the DUX4 transcript in proliferating myoblasts and FAPs.

(D) Growth rate of iDUX4(2.7) myoblasts and FAPs compared to cells from WT littermate controls. Myoblasts displayed a significant growth disadvantage. No difference was seen in FAP growth rate. One experiment of three similar replicates is shown.

(E) Immunofluorescent detection of DUX4 protein in myoblasts and myotubes. Sections are also stained with DAPI (blue) and antibody to myosin heavy chain (MHC) (in green).

(F) Quantification of DUX4+ nuclei, expressed as average percentage and SD of total per microscopic field, over 19 separate fields. One of three similar replicates is shown.

(G) Comparison of levels of DUX4 expression by RT-PCR in myoblasts versus myotubes.

See also Figure S1.

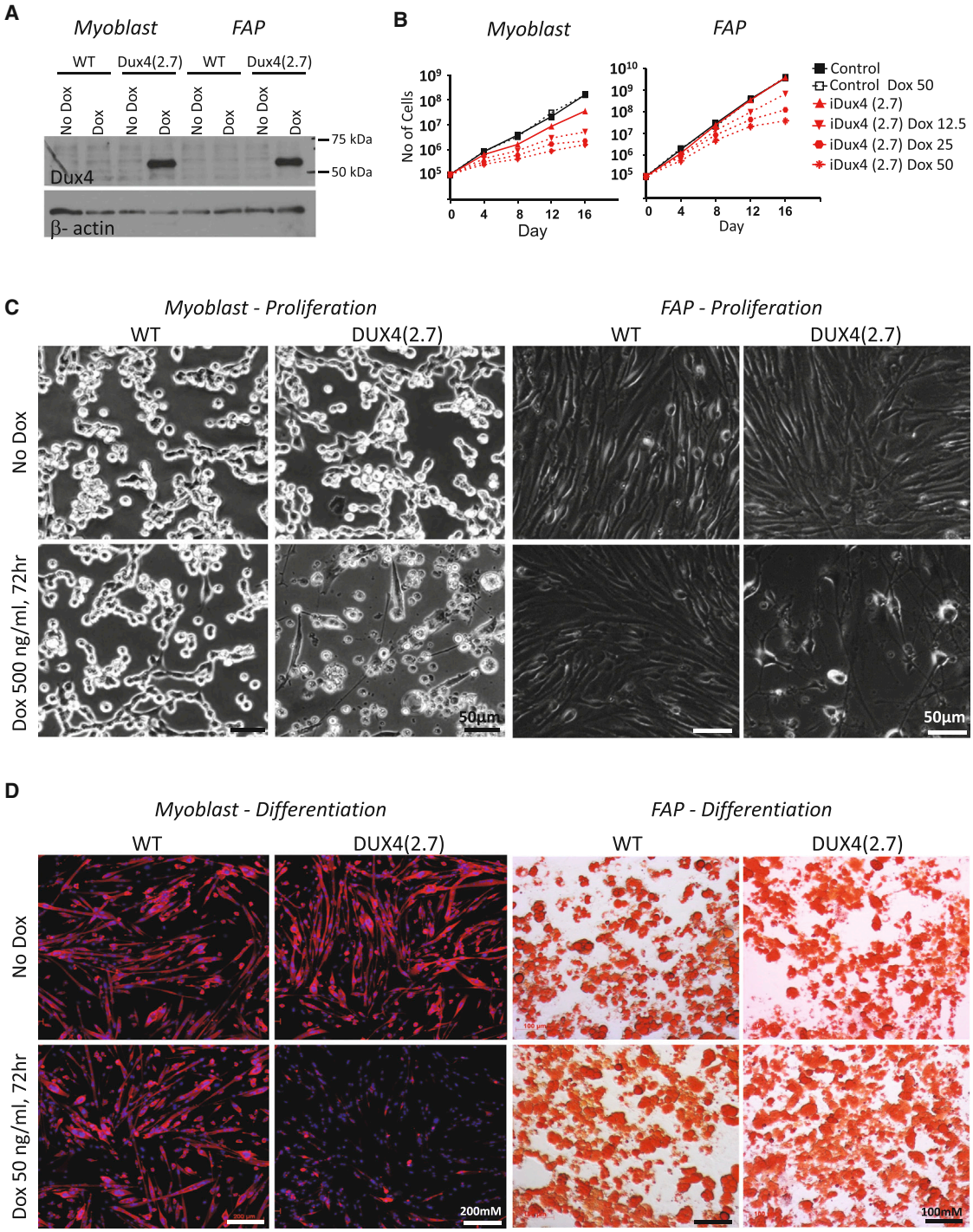


**Figure 5. Effects of Induced DUX4 Expression**

(A) Western blot for DUX4 expression in proliferating myoblasts and FAPs exposed to a high dose (500 ng/ml) of dox. One representative blot of three independent experiments is shown.

(B) Dox dose-response growth curves for myoblasts (left) and FAPs (right) exposed to very low doses of dox to induce DUX4 expression. Myoblasts displayed a more severe growth inhibition and greater sensitivity to dox.

(C) Cellular morphology of proliferating myoblast (left) and FAP (right) cultures exposed to a high dose (500 ng/ml) of dox.

(D) Myoblasts and FAPs exposed to a low dose (50 ng/ml) of dox and cultured under myogenic or adipogenic differentiation conditions, respectively. Myotubes (left) were stained for myosin heavy chain; adipocytes (right) were stained with Oil Red O. Note that low-dose induction of DUX4 inhibits myogenic, but not adipogenic, differentiation.

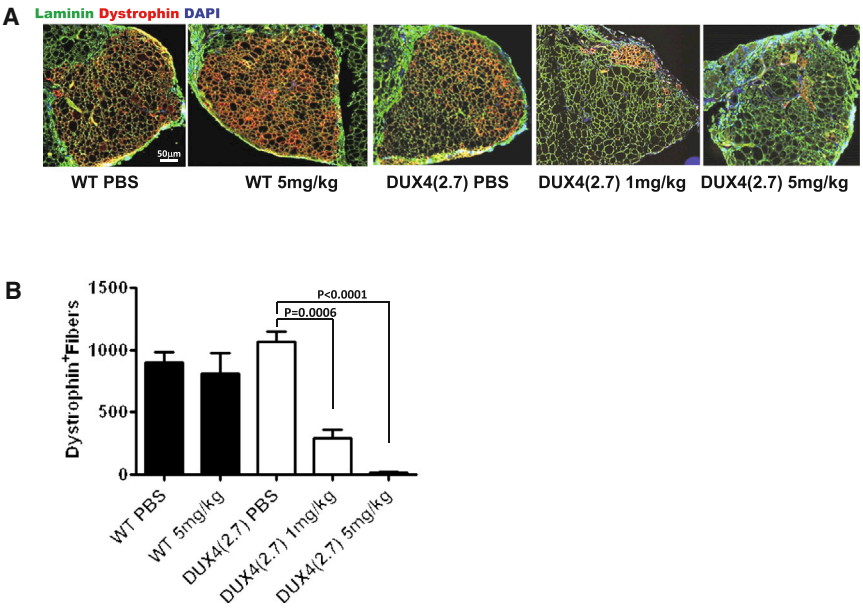


**Figure 6. DUX4 Expression Impairs Myogenic Regeneration In Vivo**

(A) Representative examples of TA muscles 1 month after transplantation of 1,800 iDUX4(2.7) satellite cells in the presence or absence of daily doxycycline injection (either 1 mg/kg or 5 mg/kg) to induce DUX4 or control carrier (PBS) injection. The overall muscle architecture is indicated by laminin staining (green). Donor cell contribution to new fibers is evaluated by counting Dystrophin+ (red) fibers. Doxycycline treatment impaired contribution to myofiber regeneration in a dose-dependent manner.

(B) Quantification of myofiber engraftment. For each group, n = 6. Bars indicate SD.

detected in humans has never been reported. With regard to pathologies in testes, this was somewhat surprising as DUX4 has been reported in human testes (Snider et al., 2010). The closest mouse homolog, Dux, was not reported expressed in testes (Clapp et al., 2007); however, a different double homeobox protein, Duxbl, which lacks the C-terminal sequence conserved between DUX4 and mouse Dux (Leidenroth and Hewitt, 2010) important for toxicity (Bosnakovski et al., 2008b), is expressed in testes (Wu et al., 2010). The presence of testis pathology in iDUX4(2.7) mice suggests that, if DUX4 has a specific function in testes, then this is probably a human-specific activity.

It is notable that the retinae of the iDUX4(2.7) animals demonstrate pathological retinal vascular changes like those seen in FSHD patients. It is not yet understood how the D4Z4 contraction leads to these changes in humans; however, it has been proposed that the muscle pathology and the retinal pathology might both be attributed to an endothelial defect (Osborne et al., 2007). The iDUX4(2.7) mice also resemble FSHD patients in terms of DUX4 expression at the RNA and protein level: a spliced mRNA encoding DUX4 can be detected at very low levels in many tissues, but the DUX4 protein itself cannot or is expressed in so few cells as to be difficult to distinguish from background in immunostaining experiments. Within the short lifespan of the rare live-born affected males, a muscular dystrophy does not develop. Whether or not muscular dystrophy (MD) would develop if the animals were to survive beyond 4–6 weeks, the absence of dystrophy is consistent with the lack of muscle pathology in young FSHD patients. The literature is inconsistent on fiber type changes in FSHD (Lin and Nonaka, 1991; Olsen et al., 2005), but neither do the mice show any signs of fiber type switching. Unlike Duchenne MD, in which pathological cycles of damage and regeneration are present from birth, FSHD muscles appear histologically normal prior to onset of the disease. The female mice do survive, but neither did they show signs of muscular dystrophy. However, in heterozygous carrier females, the DUX4 transgene appears to be predominantly on the inactive X chromosome, as it is heavily methylated. As X inactivation is random, this is best explained by positive selection for cells that silence the DUX4-bearing X chromosome.

To evaluate more directly the effect of DUX4 on primary muscle progenitors, we studied myogenic and fibroadipogenic progenitors from iDUX4(2.7) males. DUX4 mRNA was indeed expressed at low levels in both myoblasts and FAPs and was associated with a reduction in proliferative potential, more significantly to myoblasts. Doxycycline induction at high doses was clearly inhibitory to both myoblasts and FAPs, whereas low levels inhibited differentiation of myoblasts into multinucleated myotubes, but not of FAPs into adipocytes. The DUX4 effects on primary muscle progenitors raise the question of whether a defect in regeneration contributes to muscle pathology in FSHD. Accordingly, when iDUX4(2.7) satellite cells were transplanted and recipients treated with a relatively low dose of doxycycline, their ability to generate new muscle tissue was severely impaired. The data do not formally differentiate between effects on progenitors versus newly formed myofibers—certainly when very high levels of DUX4 were delivered directly to mouse muscles tissues by adeno-associated virus, there was extensive degeneration (Wallace et al., 2011). However, the data are consistent with the notion that DUX4 could impair muscle regeneration in FSHD. Most importantly, they represent a quantifiable assay that could be used to study the activity of pharmacological inhibitors of DUX4 in vivo.

This is an animal model in which FSHD allele-specific DNA has been integrated into the genome and has generated a pathological phenotype. It clearly demonstrates that even low-level expression from the terminal D4Z4 repeat is highly deleterious; is consistent with a model for FSHD in which muscle wasting is a consequence, at least in part, of impaired regeneration; and presents opportunities for testing activity of anti-DUX4 therapeutics in vivo.

## EXPERIMENTAL PROCEDURES

### Cloning of Targeting Construct and Generation of iDUX4(2.7) Mice

The genomic DNA encoding DUX4 from the terminal repeat together with downstream sequence (2.7 kb total) was obtained from pCIneo-DUX4 (Gabriëls et al., 1999) and subcloned into XhoI/NotI cloning sites of p2Lox, generating p2lox-DUX4(2.7). iDUX4(2.7)-inducible mouse embryonic stem cell

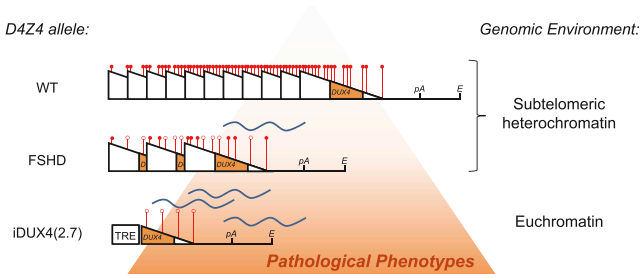


**Figure 7. The iDUX4(2.7) Allele versus Human D4Z4 Alleles**

D4Z4 is indicated by a triangle. Methylation state is indicated at six representative sites for each array, with a red ball indicating methylation and an open circle indicating lack of methylation. In humans, when D4Z4 is present in a large tandem array within subtelomeric heterochromatin at 4q, a repeat-induced silencing mechanism leads to heterochromatinization of the array (indicated by compaction of the triangles and their respective methylation marks) and hypermethylation of DNA (indicated by red circles), which effectively silences the locus. When the array number is reduced in an FSHD allele, a loss of repeat-induced silencing leads to an opening up of chromatin (more space between the triangles) and a relative demethylation, leading to some transcription of DUX4. In the iDUX4(2.7) mouse, the single copy (which is not subject to repeat-induced silencing) and location within euchromatin results in even greater opening, a complete absence of methylation, and greater transcription in additional tissues, leading to a more severe, lethal, phenotype.

(mESC) lines were generated by inducible cassette exchange recombination using an improved version of the A2Lox.cre mESC lines (ZX1 cells, which contain the second generation tetracycline-response element) as previously described (Iacovino et al., 2011). iDUX4(2.7) mice were derived at the University of Texas Southwestern Transgenic Core Facility by blastocyst injection of iDUX4(2.7) ESCs. Mice were maintained under the guidance of the University of Texas Southwestern and University of Minnesota Institutional Animal Care and Use Committees.

### RNA Isolation and RT-PCR for DUX4

RNA was isolated from fresh tissue samples dissected from iDUX4(2.7) and control male mice. Tissues were homogenized in Trizol (Invitrogen), and RNA was precipitated according to the manufacturer's directions. The high GC content of DUX4 required the use of a high-temperature reverse transcriptase. We treated 1.5 μg RNA for 30 min with DNase (Promega), and the cDNA was produced using Thermoscript polymerase and oligo dT primer according to the manufacturer's directions. DUX4 transcript was analyzed by semiquantitative PCR using Takara LA Taq with GC rich buffer II and the following conditions: primers PLH394F: GCTGGAAGCACCCCTCAGCGAGGAA and PLH395R: TCCAGGTTTGCCTAGACAGCGTC; denaturation at 94°C for 15 s; annealing at 57°C for 15 s; and elongation at 72°C for 30 s. RNA experiments were performed with at least three biological replicates, and representative results are shown.

### Statistical Analyses

GraphPad Prism was used with all samples to compute means, SDs, and p values by t test.

### Histological Analysis

Skin samples were harvested from iDUX4(2.7) and control littermates (three of each), fixed in 10% neutral buffered formalin containing 0.1 M $CaCl_2$ for 2 days, and embedded in paraffin. Four-micrometer sections were evaluated by hematoxylin and eosin (H&E) staining. Testes (from six iDUX4(2.7) and three littermate control males) were prepared in Bouin's fixative and processed for sectioning and H&E staining as described (Hao et al., 2008).

### Skeletal Muscle Contractile and Histological Analyses

EDL and soleus muscles were carefully dissected and maximal isometric force generating capacities measured. For histology, muscles were embedded in OCT. Ten-micrometer sections were evaluated by H&E staining, NADH reactivity, and myosin heavy chain expression as described (Greising et al., 2012).

### Retinal Vascular Imaging

Retinae were isolated immediately following euthanasia, fixed in Zamboni's fixative for 24 hr, washed, and stored in 20% sucrose + 0.5% sodium azide at 4°C. Whole retinae were incubated with 5% donkey serum overnight and immunostained with rat anti-CD31/PECAM-1 (Santa Cruz Biotechnology) at 1:200 dilution for 12 hr at room temperature, followed by 6 hr of washing and incubation with Cy2-conjugated secondary antibody (Jackson Immunoresearch) at 1:500 dilution for 12 hr at room temperature. Retina flat mounts were imaged using 2-micron-thick z stacks on a Fluoview FV1000 BX2 Upright Laser scanning confocal microscope (Olympus Corporation) with a 20× or 40× oil objective lens. Images were analyzed using Adobe Photoshop and Reindeer Games software to quantify different measures of retinal vasculature, as described previously (Gupta et al., 2002).

### Isolation and Differentiation of Myoblasts and FAPs from Muscle

Preparation of muscle samples was performed as described (Arpke et al., 2013). We then plated $10^6$ total mononuclear cells in a T25 flask in F-10/Ham's (Hyclone) medium containing 20% fetal bovine serum (HyClone), 50 ng/μl human basic fibroblast growth factor (Peprotech), 1% penicillin/streptomycin (Gibco), and 1% Glutamax (Gibco) and cultured at 37°C under reduced oxygen conditions (5% $O_2$, 5% $CO_2$, and 90% $N_2$). After 4 days, primary cells were disassociated with 0.05% trypsin (Invitrogen) and resuspended in FACS staining medium. To isolate myoblast and FAP fractions, cells were stained with PDGFRα conjugated with phycoerythrin (e-Biosciences; clone: APA5) and α7 integrin APC. Cells were sorted into a PDGFRα single-positive (FAP fraction) and an α7 integrin single-positive (myoblast) fraction and recultured in the same medium. Myoblasts were differentiated in 20% knockout serum replacer (Invitrogen) as described in Block et al. (2013). FAPs were differentiated in dexamethasone (STEMCELL Technologies) as described in Lemos et al. (2012). To detect DUX4 by western blot or by immunostaining in primary myoblasts and myotubes, E5-5 DUX4 antibody (Abcam) was used as described (Geng et al., 2011). Myosin heavy chain staining used the MF20 antibody (Developmental Studies Hybridoma Bank).

### Methylation Analysis

Bisulfite sequencing was generally performed as described in Hartweck et al. (2013). Tissues from six male mice at 6 weeks of age and three females aged 6, 9, and 36 weeks were analyzed. DNA was extracted using the PureLink Genomic DNA Mini Kit (Invitrogen). Five hundred nanograms DNA was converted with the EZ DNA Methylation direct kit (Zymo Research) and eluted in 20 μl. Converted DNA (2 μl) was amplified with primer sets: DR3F: GTA GAGGGGATTTTTTAATTTGTTT and DR3R: CAAACACCCCTTAACCCTAC using Takara ExTaq (QIAGEN) according to manufacturers' instructions with cycling parameters: denature: 94°C 60 s, cycle: 94°C 10 s, 60°C 15 s, 72°C 20 s, for 30 cycles; final extension at 72°C 5 min. PCR products were purified from 2% agarose gels with Wizard SVgel and PCR Purification system (Promega) cloned with the TOPO T/A cloning kit (Invitrogen) and clones with 223 bp inserts, sequenced. To determine if frequency of methylated X chromosomes with the iDux4(2.7) transgene was greater than the expected frequency (50%), we pooled the female data and used the exact binomial test. This specific PCR represents methylated and unmethylated chromosomes equally (Hartweck et al., 2013).

### Transplantation of Satellite Cells and Fiber Engraftment

Pax7-ZsGreen male mice, in which satellite cells are marked with green fluorescence (Bosnakovski et al., 2008c), were crossed to iDUX4(2.7) females to generate iDUX4(2.7); Pax7-ZsGreen males from which satellite cells were isolated by flow cytometry as described in Arpke et al. (2013). In an independent replicate that gave similar results, satellite cells were also isolated based on surface markers as described previously (Chan et al., 2013). First dead cells were gated out with propidium iodide, and then blood and endothelial lineages

were gated out using anti-CD31 (eBioscience; clone 390) and rat anti-CD45 (eBioscience; clone RA3-6B2) antibodies conjugated to phycoerythrin-Cy7. Finally, satellite cells were sorted by being double positive for CD106 (eBioscience; biotinylated primary VCAM-1 antibody; clone 429; followed by streptavidin secondary antibody conjugated with phycoerythrin) and α-7 integrin conjugated with allophycocyanin (AbLab; clone R2F2).

Transplantation was according to Arpke et al. (2013). Briefly, 2 days prior to transplantation of cells, 4-month-old NSG-mdx$^{4Cv}$ mice were anesthetized with ketamine and xylazine and both hind limbs were subjected to a 1,200 cGy dose of irradiation using an X-RAD 320 Biological Irradiator (Precision X-Ray). On the day of transplantation, 1,800 sorted satellite cells were resuspended in 1.2% $BaCl_2$ (RICCA Chemical Company) and injected into tibialis anterior (TA) muscles of NSG-mdx$^{4Cv}$ mice. Every day posttransplantation, we injected mice with PBS or doxycycline at 1 mg/kg or 5 mg/kg. Four weeks after transplantation, six TAs of each group were harvested, sectioned, and immunostained with a mouse monoclonal antibody to laminin (Sigma-Aldrich) and rabbit polyclonal antibody to dystrophin (Abcam) antibodies followed by goat anti-mouse immunoglobulin G (IgG) conjugated with Alexa 488 and goat anti-rabbit IgG conjugated with Alexa Fluor 555 (Life Science Technologies). Images were acquired on a Zeiss Axio Imager M1 Upright microscope with AxioCam HRc camera, and the number of donor-derived fibers (dystrophin+) was determined.

## SUPPLEMENTAL INFORMATION

Supplemental Information includes Supplemental Experimental Procedures and one figure and can be found with this article online at http://dx.doi.org/10.1016/j.celrep.2014.07.056.

## AUTHOR CONTRIBUTIONS

D.B. derived the iDUX4(2.7) mouse and performed initial characterization and assays for DUX4 expression with assistance from J.B. Studies of DUX4 expression and effects on differentiation of myoblasts and FAPs were performed by A.D. L.M.H. performed methylation studies. Transplantation assays were performed by A.D. and R.W.A. with assistance from R.D. K.A.B. and D.A.L. performed muscle force and fiber assays. D.V. and K.G. performed morphometric analyses of retina. F.K.H. performed analysis of testes. M.K., A.D., D.B., L.M.H., K.G., F.K.H., D.A.L., and R.C.R.P. wrote the manuscript.

## ACKNOWLEDGMENTS

This project was primarily supported by grants from the NIH (R01 AR055685), the Dr. Bob and Jean Smith Foundation, and the Friends of FSH Research to M.K. and the Muscular Dystrophy Centre Core Laboratory P30 AR0507220. D.B. was supported by a Muscular Dystrophy Association Development Grant (MDA 4361) and a Marjorie Bronfman Research Fellowship from the FSH Society (FSHS-MGBF-016). R.C.R.P. was supported by NIH grants R01 AR055299 and U01 HL100407. K.A.B. was supported by NIH grant T32-AR07612 and D.A.L. by K02-AG036827. K.G. and D.V. were supported by NIH grants R01 HL68802 and R01 HL103773. F.K.H. was supported by NIH grant R01 HD053889.

Received: December 20, 2013
Revised: June 3, 2014
Accepted: July 30, 2014
Published: August 28, 2014

## REFERENCES

Agha-Mohammadi, S., O'Malley, M., Etemad, A., Wang, Z., Xiao, X., and Lotze, M.T. (2004). Second-generation tetracycline-regulatable promoter: repositioned tet operator elements optimize transactivator synergy while shorter minimal promoter offers tight basal leakiness. J. Gene Med. *6*, 817–828.

Arpke, R.W., Darabi, R., Mader, T.L., Zhang, Y., Toyama, A., Lonetree, C.L., Nash, N., Lowe, D.A., Perlingeiro, R.C., and Kyba, M. (2013). A new immuno-, dystrophin-deficient model, the NSG-mdx(4Cv) mouse, provides evidence for functional improvement following allogeneic satellite cell transplantation. Stem Cells *31*, 1611–1620.

Bakker, E., Wijmenga, C., Vossen, R.H., Padberg, G.W., Hewitt, J., van der Wielen, M., Rasmussen, K., and Frants, R.R. (1995). The FSHD-linked locus D4F104S1 (p13E-11) on 4q35 has a homologue on 10qter. Muscle Nerve Suppl. *2*, S39–S44.

Block, G.J., Narayanan, D., Amell, A.M., Petek, L.M., Davidson, K.C., Bird, T.D., Tawil, R., Moon, R.T., and Miller, D.G. (2013). Wnt/β-catenin signaling suppresses DUX4 expression and prevents apoptosis of FSHD muscle cells. Hum. Mol. Genet. *22*, 4661–4672.

Bosnakovski, D., Xu, Z., Gang, E.J., Galindo, C.L., Liu, M., Simsek, T., Garner, H.R., Agha-Mohammadi, S., Tassin, A., Coppée, F., et al. (2008a). An isogenetic myoblast expression screen identifies DUX4-mediated FSHD-associated molecular pathologies. EMBO J. *27*, 2766–2779.

Bosnakovski, D., Lamb, S., Simsek, T., Xu, Z., Belayew, A., Perlingeiro, R., and Kyba, M. (2008b). DUX4c, an FSHD candidate gene, interferes with myogenic regulators and abolishes myoblast differentiation. Exp. Neurol. *214*, 87–96.

Bosnakovski, D., Xu, Z., Li, W., Thet, S., Cleaver, O., Perlingeiro, R.C., and Kyba, M. (2008c). Prospective isolation of skeletal muscle stem cells with a Pax7 reporter. Stem Cells *26*, 3194–3204.

Bronson, S.K., Plaehn, E.G., Kluckman, K.D., Hagaman, J.R., Maeda, N., and Smithies, O. (1996). Single-copy transgenic mice with chosen-site integration. Proc. Natl. Acad. Sci. USA *93*, 9067–9072.

Brouwer, O.F., Padberg, G.W., Ruys, C.J., Brand, R., de Laat, J.A., and Grote, J.J. (1991). Hearing loss in facioscapulohumeral muscular dystrophy. Neurology *41*, 1878–1881.

Celegato, B., Capitanio, D., Pescatori, M., Romualdi, C., Pacchioni, B., Cagnin, S., Viganò, A., Colantoni, L., Begum, S., Ricci, E., et al. (2006). Parallel protein and transcript profiles of FSHD patient muscles correlate to the D4Z4 arrangement and reveal a common impairment of slow to fast fibre differentiation and a general deregulation of MyoD-dependent genes. Proteomics *6*, 5303–5321.

Chan, S.S., Shi, X., Toyama, A., Arpke, R.W., Dandapat, A., Iacovino, M., Kang, J., Le, G., Hagen, H.R., Garry, D.J., and Kyba, M. (2013). Mesp1 patterns mesoderm into cardiac, hematopoietic, or skeletal myogenic progenitors in a context-dependent manner. Cell Stem Cell *12*, 587–601.

Chen, T.H., Lai, Y.H., Lee, P.L., Hsu, J.H., Goto, K., Hayashi, Y.K., Nishino, I., Lin, C.W., Shih, H.H., Huang, C.C., et al. (2013). Infantile facioscapulohumeral muscular dystrophy revisited: Expansion of clinical phenotypes in patients with a very short EcoRI fragment. Neuromuscul. Disord. *23*, 298–305.

Clapp, J., Mitchell, L.M., Bolland, D.J., Fantes, J., Corcoran, A.E., Scotting, P.J., Armour, J.A., and Hewitt, J.E. (2007). Evolutionary conservation of a coding function for D4Z4, the tandem DNA repeat mutated in facioscapulohumeral muscular dystrophy. Am. J. Hum. Genet. *81*, 264–279.

Cvetkovic, B., Yang, B., Williamson, R.A., and Sigmund, C.D. (2000). Appropriate tissue- and cell-specific expression of a single copy human angiotensinogen transgene specifically targeted upstream of the HPRT locus by homologous recombination. J. Biol. Chem. *275*, 1073–1078.

de Greef, J.C., Lemmers, R.J., van Engelen, B.G., Sacconi, S., Venance, S.L., Frants, R.R., Tawil, R., and van der Maarel, S.M. (2009). Common epigenetic changes of D4Z4 in contraction-dependent and contraction-independent FSHD. Hum. Mutat. *30*, 1449–1459.

Deidda, G., Cacurri, S., Piazzo, N., and Felicetti, L. (1996). Direct detection of 4q35 rearrangements implicated in facioscapulohumeral muscular dystrophy (FSHD). J. Med. Genet. *33*, 361–365.

Dixit, M., Ansseau, E., Tassin, A., Winokur, S., Shi, R., Qian, H., Sauvage, S., Mattéotti, C., van Acker, A.M., Leo, O., et al. (2007). DUX4, a candidate gene of facioscapulohumeral muscular dystrophy, encodes a transcriptional activator of PITX1. Proc. Natl. Acad. Sci. USA *104*, 18157–18162.

Fitzsimons, R.B., Gurwin, E.B., and Bird, A.C. (1987). Retinal vascular abnormalities in facioscapulohumeral muscular dystrophy. A general association with genetic and therapeutic implications. Brain *110*, 631–648.

Gabellini, D., Green, M.R., and Tupler, R. (2002). Inappropriate gene activation in FSHD: a repressor complex binds a chromosomal repeat deleted in dystrophic muscle. Cell *110*, 339–348.

Gabriëls, J., Beckers, M.C., Ding, H., De Vriese, A., Plaisance, S., van der Maarel, S.M., Padberg, G.W., Frants, R.R., Hewitt, J.E., Collen, D., and Belayew, A. (1999). Nucleotide sequence of the partially deleted D4Z4 locus in a patient with FSHD identifies a putative gene within each 3.3 kb element. Gene *236*, 25–32.

Geng, L.N., Tyler, A.E., and Tapscott, S.J. (2011). Immunodetection of human double homeobox 4. Hybridoma (Larchmt) *30*, 125–130.

Gieron, M.A., Korthals, J.K., and Kousseff, B.G. (1985). Facioscapulohumeral dystrophy with cochlear hearing loss and tortuosity of retinal vessels. Am. J. Med. Genet. *22*, 143–147.

Greising, S.M., Call, J.A., Lund, T.C., Blazar, B.R., Tolar, J., and Lowe, D.A. (2012). Skeletal muscle contractile function and neuromuscular performance in Zmpste24 -/- mice, a murine model of human progeria. Age (Dordr.) *34*, 805–819.

Gupta, K., Kshirsagar, S., Chang, L., Schwartz, R., Law, P.Y., Yee, D., and Hebbel, R.P. (2002). Morphine stimulates angiogenesis by activating proangiogenic and survival-promoting signaling and promotes breast tumor growth. Cancer Res. *62*, 4491–4498.

Hao, J., Yamamoto, M., Richardson, T.E., Chapman, K.M., Denard, B.S., Hammer, R.E., Zhao, G.Q., and Hamra, F.K. (2008). Sohlh2 knockout mice are male-sterile because of degeneration of differentiating type A spermatogonia. Stem Cells *26*, 1587–1597.

Hartweck, L.M., Anderson, L.J., Lemmers, R.J., Dandapat, A., Toso, E.A., Dalton, J.C., Tawil, R., Day, J.W., van der Maarel, S.M., and Kyba, M. (2013). A focal domain of extreme demethylation within D4Z4 in FSHD2. Neurology *80*, 392–399.

Hochedlinger, K., Yamada, Y., Beard, C., and Jaenisch, R. (2005). Ectopic expression of Oct-4 blocks progenitor-cell differentiation and causes dysplasia in epithelial tissues. Cell *121*, 465–477.

Iacovino, M., Bosnakovski, D., Fey, H., Rux, D., Bajwa, G., Mahen, E., Mitanoska, A., Xu, Z., and Kyba, M. (2011). Inducible cassette exchange: a rapid and efficient system enabling conditional gene expression in embryonic stem and primary cells. Stem Cells *29*, 1580–1588.

Joe, A.W., Yi, L., Natarajan, A., Le Grand, F., So, L., Wang, J., Rudnicki, M.A., and Rossi, F.M. (2010). Muscle injury activates resident fibro/adipogenic progenitors that facilitate myogenesis. Nat. Cell Biol. *12*, 153–163.

Jones, T.I., Chen, J.C., Rahimov, F., Homma, S., Arashiro, P., Beermann, M.L., King, O.D., Miller, J.B., Kunkel, L.M., Emerson, C.P., Jr., et al. (2012). Facioscapulohumeral muscular dystrophy family studies of DUX4 expression: evidence for disease modifiers and a quantitative model of pathogenesis. Hum. Mol. Genet. *21*, 4419–4430.

Kowaljow, V., Marcowycz, A., Ansseau, E., Conde, C.B., Sauvage, S., Mattéotti, C., Arias, C., Corona, E.D., Nuñez, N.G., Leo, O., et al. (2007). The DUX4 gene at the FSHD1A locus encodes a pro-apoptotic protein. Neuromuscul. Disord. *17*, 611–623.

Krom, Y.D., Thijssen, P.E., Young, J.M., den Hamer, B., Balog, J., Yao, Z., Maves, L., Snider, L., Knopp, P., Zammit, P.S., et al. (2013). Intrinsic epigenetic regulation of the D4Z4 macrosatellite repeat in a transgenic mouse model for FSHD. PLoS Genet. *9*, e1003415.

Leidenroth, A., and Hewitt, J.E. (2010). A family history of DUX4: phylogenetic analysis of DUXA, B, C and Duxbl reveals the ancestral DUX gene. BMC Evol. Biol. *10*, 364.

Lemmers, R.J., Wohlgemuth, M., Frants, R.R., Padberg, G.W., Morava, E., and van der Maarel, S.M. (2004). Contractions of D4Z4 on 4qB subtelomeres do not cause facioscapulohumeral muscular dystrophy. Am. J. Hum. Genet. *75*, 1124–1130.

Lemmers, R.J., Wohlgemuth, M., van der Gaag, K.J., van der Vliet, P.J., van Teijlingen, C.M., de Knijff, P., Padberg, G.W., Frants, R.R., and van der Maarel, S.M. (2007). Specific sequence variations within the 4q35 region are associated with facioscapulohumeral muscular dystrophy. Am. J. Hum. Genet. *81*, 884–894.

Lemmers, R.J., van der Vliet, P.J., Klooster, R., Sacconi, S., Camaño, P., Dauwerse, J.G., Snider, L., Straasheijm, K.R., van Ommen, G.J., Padberg, G.W., et al. (2010). A unifying genetic model for facioscapulohumeral muscular dystrophy. Science *329*, 1650–1653.

Lemmers, R.J., Tawil, R., Petek, L.M., Balog, J., Block, G.J., Santen, G.W., Amell, A.M., van der Vliet, P.J., Almomani, R., Straasheijm, K.R., et al. (2012). Digenic inheritance of an SMCHD1 mutation and an FSHD-permissive D4Z4 allele causes facioscapulohumeral muscular dystrophy type 2. Nat. Genet. *44*, 1370–1374.

Lemos, D.R., Paylor, B., Chang, C., Sampaio, A., Underhill, T.M., and Rossi, F.M. (2012). Functionally convergent white adipogenic progenitors of different lineages participate in a diffused system supporting tissue regeneration. Stem Cells *30*, 1152–1162.

Lin, M.Y., and Nonaka, I. (1991). Facioscapulohumeral muscular dystrophy: muscle fiber type analysis with particular reference to small angular fibers. Brain Dev. *13*, 331–338.

Lutz, K.L., Holte, L., Kliethermes, S.A., Stephan, C., and Mathews, K.D. (2013). Clinical and genetic features of hearing loss in facioscapulohumeral muscular dystrophy. Neurology *81*, 1374–1377.

Olsen, D.B., Ørngreen, M.C., and Vissing, J. (2005). Aerobic training improves exercise performance in facioscapulohumeral muscular dystrophy. Neurology *64*, 1064–1066.

Osborne, R.J., Welle, S., Venance, S.L., Thornton, C.A., and Tawil, R. (2007). Expression profile of FSHD supports a link between retinal vasculopathy and muscular dystrophy. Neurology *68*, 569–577.

Padberg, G.W., Brouwer, O.F., de Keizer, R.J., Dijkman, G., Wijmenga, C., Grote, J.J., and Frants, R.R. (1995). On the significance of retinal vascular disease and hearing loss in facioscapulohumeral muscular dystrophy. Muscle Nerve Suppl. *2*, S73–S80.

Portales-Casamar, E., Swanson, D.J., Liu, L., de Leeuw, C.N., Banks, K.G., Ho Sui, S.J., Fulton, D.L., Ali, J., Amirabbasi, M., Arenillas, D.J., et al. (2010). A regulatory toolbox of MiniPromoters to drive selective expression in the brain. Proc. Natl. Acad. Sci. USA *107*, 16589–16594.

Small, R.G. (1968). Coats' disease and muscular dystrophy. Trans. Am. Acad. Ophthalmol. Otolaryngol. *72*, 225–231.

Snider, L., Asawachaicharn, A., Tyler, A.E., Geng, L.N., Petek, L.M., Maves, L., Miller, D.G., Lemmers, R.J., Winokur, S.T., Tawil, R., et al. (2009). RNA transcripts, miRNA-sized fragments and proteins produced from D4Z4 units: new candidates for the pathophysiology of facioscapulohumeral dystrophy. Hum. Mol. Genet. *18*, 2414–2430.

Snider, L., Geng, L.N., Lemmers, R.J., Kyba, M., Ware, C.B., Nelson, A.M., Tawil, R., Filippova, G.N., van der Maarel, S.M., Tapscott, S.J., and Miller, D.G. (2010). Facioscapulohumeral dystrophy: incomplete suppression of a retrotransposed gene. PLoS Genet. *6*, e1001181.

Tassin, A., Laoudj-Chenivesse, D., Vanderplanck, C., Barro, M., Charron, S., Ansseau, E., Chen, Y.W., Mercier, J., Coppée, F., and Belayew, A. (2013). DUX4 expression in FSHD muscle cells: how could such a rare protein cause a myopathy? J. Cell. Mol. Med. *17*, 76–89.

Touw, K., Hoggatt, A.M., Simon, G., and Herring, B.P. (2007). Hprt-targeted transgenes provide new insights into smooth muscle-restricted promoter activity. Am. J. Physiol. Cell Physiol. *292*, C1024–C1032.

Turki, A., Hayot, M., Carnac, G., Pillard, F., Passerieux, E., Bommart, S., Raynaud de Mauverger, E., Hugon, G., Pincemail, J., Pietri, S., et al. (2012). Functional muscle impairment in facioscapulohumeral muscular dystrophy is correlated with oxidative stress and mitochondrial dysfunction. Free Radic. Biol. Med. *53*, 1068–1079.

Uezumi, A., Fukada, S., Yamamoto, N., Takeda, S., and Tsuchida, K. (2010). Mesenchymal progenitors distinct from satellite cells contribute to ectopic fat cell formation in skeletal muscle. Nat. Cell Biol. *12*, 143–152.

van Deutekom, J.C., Wijmenga, C., van Tienhoven, E.A., Gruter, A.M., Hewitt, J.E., Padberg, G.W., van Ommen, G.J., Hofker, M.H., and Frants, R.R. (1993).

FSHD associated DNA rearrangements are due to deletions of integral copies of a 3.2 kb tandemly repeated unit. Hum. Mol. Genet. *2*, 2037–2042.

van Overveld, P.G., Lemmers, R.J., Sandkuijl, L.A., Enthoven, L., Winokur, S.T., Bakels, F., Padberg, G.W., van Ommen, G.J., Frants, R.R., and van der Maarel, S.M. (2003). Hypomethylation of D4Z4 in 4q-linked and non-4q-linked facioscapulohumeral muscular dystrophy. Nat. Genet. *35*, 315–317.

Wallace, L.M., Garwick, S.E., Mei, W., Belayew, A., Coppee, F., Ladner, K.J., Guttridge, D., Yang, J., and Harper, S.Q. (2011). DUX4, a candidate gene for facioscapulohumeral muscular dystrophy, causes p53-dependent myopathy in vivo. Ann. Neurol. *69*, 540–552.

Wijmenga, C., Hewitt, J.E., Sandkuijl, L.A., Clark, L.N., Wright, T.J., Dauwerse, H.G., Gruter, A.M., Hofker, M.H., Moerer, P., Williamson, R., et al. (1992). Chromosome 4q DNA rearrangements associated with facioscapulohumeral muscular dystrophy. Nat. Genet. *2*, 26–30.

Winokur, S.T., Chen, Y.W., Masny, P.S., Martin, J.H., Ehmsen, J.T., Tapscott, S.J., van der Maarel, S.M., Hayashi, Y., and Flanigan, K.M. (2003a). Expression profiling of FSHD muscle supports a defect in specific stages of myogenic differentiation. Hum. Mol. Genet. *12*, 2895–2907.

Winokur, S.T., Barrett, K., Martin, J.H., Forrester, J.R., Simon, M., Tawil, R., Chung, S.A., Masny, P.S., and Figlewicz, D.A. (2003b). Facioscapulohumeral muscular dystrophy (FSHD) myoblasts demonstrate increased susceptibility to oxidative stress. Neuromuscul. Disord. *13*, 322–333.

Wu, S.L., Tsai, M.S., Wong, S.H., Hsieh-Li, H.M., Tsai, T.S., Chang, W.T., Huang, S.L., Chiu, C.C., and Wang, S.H. (2010). Characterization of genomic structures and expression profiles of three tandem repeats of a mouse double homeobox gene: Duxbl. Dev. Dyn. *239*, 927–940.

Zeng, W., de Greef, J.C., Chen, Y.Y., Chien, R., Kong, X., Gregson, H.C., Winokur, S.T., Pyle, A., Robertson, K.D., Schmiesing, J.A., et al. (2009). Specific loss of histone H3 lysine 9 trimethylation and HP1gamma/cohesin binding at D4Z4 repeats is associated with facioscapulohumeral dystrophy (FSHD). PLoS Genet. *5*, e1000559.